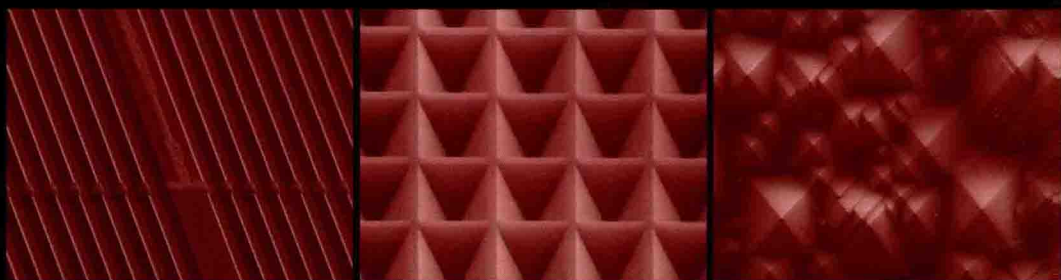




Amorphous Silicon / Crystalline Silicon Heterojunction Solar Cells

非晶硅/晶体硅异质结太阳电池

[德] Wolfgang Rainer Fahrner (沃尔夫冈·瑞纳·法赫纳) 主编



化学工业出版社
Chemical Industry Press

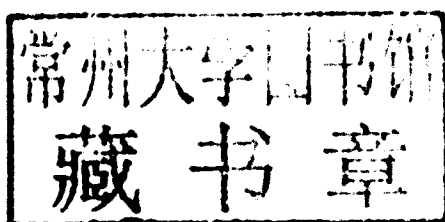


Springer

Amorphous Silicon / Crystalline Silicon Heterojunction Solar Cells

非晶硅/晶体硅异质结太阳电池

[德] Wolfgang Rainer Fahrner (沃尔夫冈·瑞纳·法赫纳) 主编



化学工业出版社
Chemical Industry Press

· 北 京 ·

非晶硅/晶体硅异质结太阳能电池 (Amorphous Silicon/Crystalline Silicon Heterojunction Solar Cells) 是太阳能电池中深具代表性的一类, 具有开路电压高、填充因子高、转换效率高等优点, 具有广阔的技术进步空间和市场发展前景。

本书介绍了非晶硅/晶体硅异质结太阳能电池的基本结构和制备技术, 讨论了其市场潜力, 概述了非晶硅/晶体硅异质结太阳能电池的发展历史, 论述了其构成材料及能带结构, 分步详解了其制备工艺, 包括抛光、腐蚀、制绒、本征层、背电场、减反射层及金属层沉积等; 本书还对其结构的合理性进行了论证。非晶硅/晶体硅异质结太阳能电池现阶段的主要问题及挑战有: 基础材料的选择、n/p 结构或者 p/n 结构的选择, 表面缺陷态、晶硅表面钝化效果的优化、发射极和背电场层。对于测试分析技术, 本书部分列举了反射、透过、微波测试技术、光学及光电测试、椭偏仪、拉曼光谱、光/暗 IV 曲线、量子效率、光诱导电流等。本书还采用 AFORS-HET 软件模拟分析太阳能电池的性能并与实验相比较验证, 并对非晶硅/晶体硅异质结太阳能电池的衰减特性和耐辐射特性进行了测试。本书结尾列举了当前实验室研究所获得的最优太阳能电池效率和中国目前相关研究和产业现状。

本书可供从事新能源材料、太阳能光伏以及半导体材料等领域的科技工作者和企业工程师作为参考, 也可作为大专院校相关专业师生的教学参考书。

图书在版编目 (CIP) 数据

非晶硅/晶体硅异质结太阳能电池=Amorphous Silicon/Crystalline Silicon Heterojunction Solar Cells: 英文/(德)法赫纳 (Fahrner W.R.) 主编.—北京: 化学工业出版社, 2014.5
ISBN 978-7-122-15935-9

I. ①非… II. ①法… III. ①硅太阳能电池-英文
IV. ①TM914.4

中国版本图书馆 CIP 数据核字 (2012) 第 286929 号

本书由化学工业出版社与 Springer 出版公司合作出版。版权由化学工业出版社所有。本版本仅供中国内地销售, 不可销往香港、澳门和台湾。

责任编辑: 朱 彤 吴 刚

装帧设计: 刘丽华

出版发行: 化学工业出版社 (北京市东城区青年湖南街 13 号 邮政编码 100011)
印 刷: 北京永鑫印刷有限责任公司
装 订: 三河市万龙印装有限公司
710mm×1000mm 1/16 印张 7 1/2 字数 133 千字 2014 年 6 月北京第 1 版第 1 次印刷

购书咨询: 010-64518888 (传真: 010-64519686) 售后服务: 010-64518899
网 址: <http://www.cip.com.cn>
凡购买本书, 如有缺损质量问题, 本社销售中心负责调换。

定 价: 98.00

版权所有 违者必究

Amorphous Silicon / Crystalline Silicon Heterojunction Solar Cells 非晶硅/晶体硅异质结太阳能电池

Contributor List (作者名单)

Wolfgang R. Fahrner ^{*,1, 2}, **Haibin Huang** ², **Thomas Mueller** ¹,
Stefan Schwertheim ¹, **Frank Wuensch** ¹, and **Heinz-Christoph
Neitzert** ³

1 University of Hagen, Chair of Electronic Devices, Haldener Str. 182, D-58084 Hagen, Germany

2 Nanchang University, School of Photovoltaics, Xuefu Ave. 999, 330031 Nanchang, China

3 University of Salerno, Via Ponte Don Melillo 1, 84084 Fisciano (SA), Italy
E-Mails: thomas.mueller@nus.edu.sg (T.M.); haibinhuang@ncu.edu.cn (H.H);
s.schwertheim@web.de (S.S.); Frank.Wuensch@alumni.TU-Berlin.de (F.W.);
neitzert@unisa.it (H.C.N.)

* Author to whom correspondence should be addressed; E-Mail:
wolfgang.fahrner@fernuni-hagen.de;

Tel.: +49-761-551

Fax: +49-762-12017230,

Preface

The need to replace conventional energies—coal, oil and nuclear power—by alternative ones has been emphasised many times and underlined only recently in the Durban Climate Change Conference. Among these alternatives, photovoltaic devices play a leading role. This book here deals with one important representative, the heterojunction solar cell.

As its name points out, it consists of two different materials, crystalline and amorphous silicon. While the former one was brought to a high standard already shortly after World War II, amorphous silicon was investigated in detail only in 1968, in Romania. In contrast, heterojunction solar cell production of today is a flourishing business as seen by the example of Sanyo or Meyer Burger.

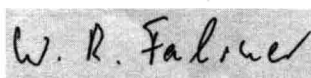
This book deals with some typical properties of the heterojunction cell. Its history, schematic cross-sections, and production tools will be shown. A special chapter is devoted to the challenges of the cell such as texturization, interface defects, passivation, lifetime and surface velocity, epitaxial layer formation, emitter, and back surface field conductivity.

Some important measurement tools are presented.

Today no electronic device will be produced any more before it is not simulated. Thus, we present a few of the simulation programmes available on the market.

The book is completed with a brief survey of the state of the art as represented by the efficiencies.

Because China is the strongest emerging market in the solar cell field a collection of related publications and their discussion appeared to be mandatory.



Nanchang, December 2011

Wolfgang Rainer Fahrner

Acknowledgments

The authors thank Mrs. K. Meusinger and Dipl.-Ing. B. Wdowiak, University of Hagen, for technical assistance, A. Denker, affiliated to the Helmholtz Zentrum Berlin (HZB) (formerly Hahn-Meitner Institut Berlin (HMI)) and B. Limata, M. Romano and L. Gialanella from the Physics Department of Naples University for the proton irradiation, R. Scheer (HZB) for the EBIC measurements and M. Ferrara affiliated to the ENEA research center in Portici for the electroluminescence measurements. The authors gratefully acknowledge the fruitful discussions with M. Kunst (HZB).

Contributors

Wolfgang Rainer Fahrner Chair of Electronic Devices, University of Hagen, Haldener Str. 182, 58084 Hagen, Germany; School of Photovoltaic Engineering, Nanchang University, Xuefu Ave. 999, 330031 Nanchang, China, e-mail: wolfgang.fahrner@fernuni-hagen.de

Haibin Huang School of Photovoltaic Engineering, Nanchang University, Xuefu Ave. 999, 330031 Nanchang, China, e-mail: Haibinhuang@ncu.edu.cn

Thomas Mueller Chair of Electronic Devices, University of Hagen, Haldener Str. 182, 58084 Hagen, Germany, e-mail: thomas.mueller@nus.edu.sg

Stefan Schwertheim Chair of Electronic Devices, University of Hagen, Haldener Str. 182, 58084 Hagen, Germany, e-mail: s.schwertheim@web.de

Frank Wuensch Chair of Electronic Devices, University of Hagen, Haldener Str. 182, 58084 Hagen, Germany, e-mail: Frank.Wuensch@alumni.TU-Berlin.de

Heinz-Christoph Neitzert University of Salerno, Via Ponte Don Melillo 1, 84084 Fisciano, SA, Italy, e-mail: neitzert@unisa.it

Contents

Amorphous Silicon / Crystalline Silicon Heterojunction Solar Cells. . .	1
1 Introduction.	1
1.1 Basic Structure.	1
1.2 History of a-Si:H/c-Si Device Development.	3
1.3 Economic Aspects	6
2 Useful Material Parameters	7
2.1 Useful Data of Monocrystalline Silicon.	7
2.2 Useful Data of Multicrystalline Silicon	9
2.3 Useful Data of Microcrystalline Silicon.	9
2.4 Useful Data of Amorphous Silicon with Respect to Heterojunction Solar Cells	11
3 Manufacturing	14
3.1 Lapping and Polishing.	14
3.2 Texturing.	14
3.3 Cleaning	17
3.4 PECVD of i-, n-, and p-Layers.	17
3.5 TCO	19
3.6 Metallization and Screen Printing	19
4 Concepts.	21
4.1 Conventional n a-Si:H/p c-Si Cell.	21
4.2 Bifacial a-Si:H/c-Si Heterojunction Solar Cell with Intrinsic Thin Layer, HIT Structure	22
4.3 a-Si:H/c-Si Heterocontact Cell Without i-Layer	22
4.4 Other Concepts for Improved Entrance Windows.	23
4.5 a-Si:H/c-Si Heterocontact Cell with Inverted Geometry.	23
4.6 Interdigitated HIT Cell	24
5 Problems and Challenges	25
5.1 Choice of the Base Material, Impact of the Doping, n/p Versus p/n	25
5.2 Surface States	26
5.3 Surface Passivation.	28
5.4 PECV-Deposited Emitter and Back Surface Field.	34

6	Measurement Techniques	37
6.1	Absorption, Reflection, and Transmission	37
6.2	Excess Charge Carrier Lifetime	38
6.3	Electroluminescence	49
6.4	a-Si Characterization	50
6.5	Electronic Device Characterization	55
7	Simulation.	58
7.1	AFORS-HET	59
7.2	Comparison with Experiments	60
8	Long-Term Stability and Degradation.	64
8.1	Long-Term Stability	64
8.2	Radiation Hardness	65
9	State of the Art	78
10	Silicon-Based Heterojunction Solar Cells in China.	78
10.1	Introduction of the Active Groups in this Area in China	79
10.2	Experimental Studies	80
10.3	Theoretical Simulation	94
	References	99

Amorphous Silicon / Crystalline Silicon Heterojunction Solar Cells

Wolfgang Rainer Fahrner

1 Introduction

1.1 Basic Structure

Like any other (semiconductor) solar cell, the amorphous silicon / crystalline silicon heterojunction solar cell consists of a combination of p-type and n-type material, that is, a diode structure. However, while in the usual case the n-type and the p-type semiconductors are identical and just differ in the doping, a heterojunction is built on two different materials, crystalline and amorphous silicon in our case. Its basic structure is given in Fig. 1.

A crystalline wafer acts as a substrate for the amorphous layer on its top. In the following, the abbreviations c-Si and a-Si are used for crystalline and amorphous silicon, respectively. To obtain the required diode structure, it is evident that the two materials must be of opposite doping type. The amorphous layer acts as emitter and the wafer as the base of the solar cell.

During the development of the heterojunction cell, the range of emitter and base materials has been expanded. For instance, the initially monocrystalline silicon had been replaced by multicrystalline material of various origins (edge-defined ribbon growth, block-cast silicon, etc.). Similarly, microcrystalline silicon had been tried instead of amorphous silicon.

Of course, a cell according to Fig. 1 would not operate very efficiently. For instance, incoming light would be reflected to a good deal. As a first countermeasure, an antireflection coating (ARC, cf. Sect. 3.2) is deposited on the a-Si. The ARC is highly transparent and highly conductive. Together with a texture

W. R. Fahrner (✉)

Chair of Electronic Devices, University of Hagen, Haldener 182, 58084 Hagen, Germany
e-mail: wolfgang.fahrner@fernuni-hagen.de

W. R. Fahrner

School of Photovoltaic Engineering, Nanchang University, Xuefu Ave. 999, 330031
Nanchang, China

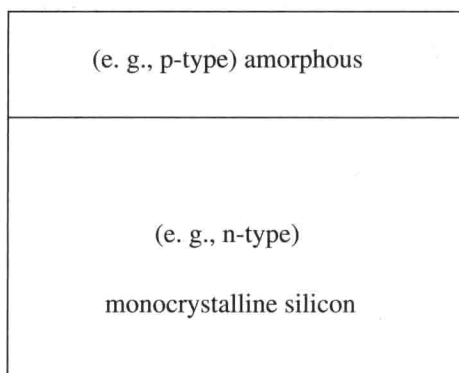


Fig. 1 Basic structure of the amorphous silicon / crystalline silicon heterojunction solar cell

(roughening of the surface, cf. Sect. 3.2), reflection is almost totally suppressed. Furthermore, we need electrical contacts. The usual solution is an array of metallic fingers mutually connected by a busbar on the front side and a metal back contact. However, other solutions with interdigitated contacts at the rear are known (cf. Sect. 4.2). The application of a conductive ARC serves a second purpose, namely the improved lateral transport of carriers generated between the fingers. The a-Si alone offers a very low conductance. Finally, the surfaces of the wafer must not be neglected. The c-Si surfaces are full of so-called surface (or interface) states yielding a high recombination and loss in current gain. Thus, it is advisable to deposit a thin intrinsic layer on either surface of the wafer (cf. Sect. 5.3). As a rule, the deposition of the backside intrinsic layer is followed by another deposition, namely the so-called back surface field (BSF) layer. The BSF repels minority carriers trying to reach the recombination centers at the back contact.

Summing up all these improvements, we end up with a cross section of Fig. 2.

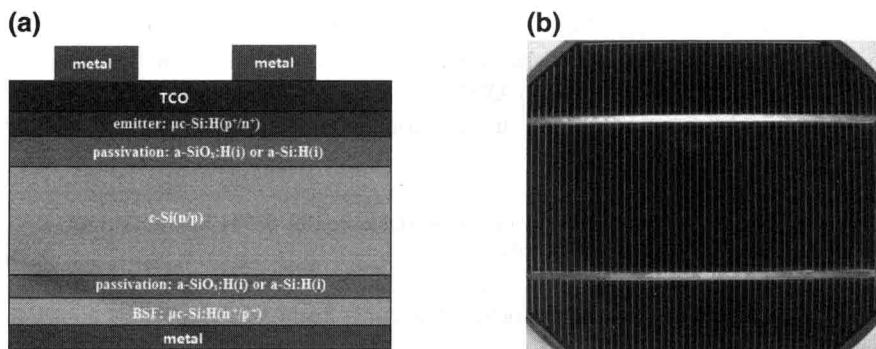


Fig. 2 **a** Improved structure (*left*), texture not shown and **b** a photograph of a typical solar cell (*right*)

Typical geometrical data of the solar cell are Area of 100×100 mm, wafer thickness of $210 \mu\text{m}$, finger width of $150 \mu\text{m}$, finger distance (center to center) of 2 mm, busbar width of 2 mm, busbar distance (center to center) of 50 mm, intrinsic layer thicknesses of 5–10 nm, indium tin oxide layer (as ARC) of 80 nm, emitter layer of 5–10 nm, and the metallization on the back side of a few μm .

1.2 History of a-Si:H/c-Si Device Development

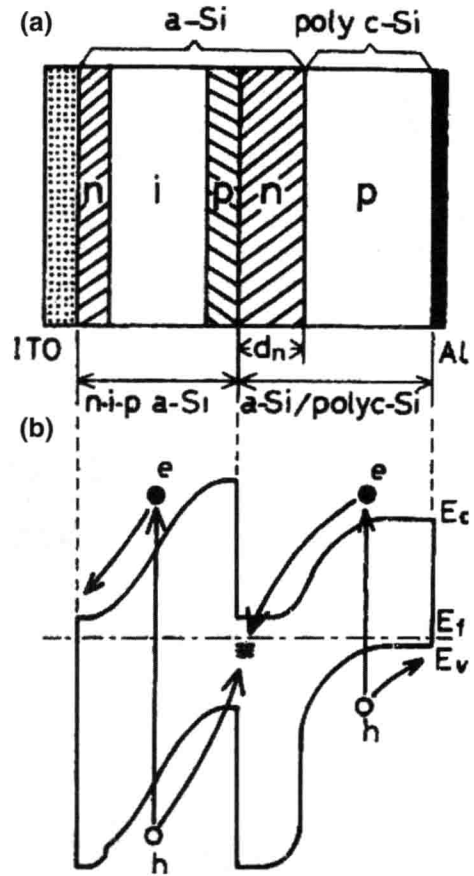
The investigation of the heterojunction between amorphous silicon and crystalline silicon started more than 40 years ago. The first-reported a-Si/c-Si heterojunction has been published by Grigorivici et al. [1], by evaporation of amorphous non-hydrogenated silicon at room temperature on top of n-type or p-type crystalline silicon with different resistivities and successive annealing of the deposited films at temperatures of either 290 or 500 °C [1]. This deposition method resulted in a highly defective amorphous silicon layer, and the study aimed to determine the transport mechanism in the amorphous silicon layer. The authors concluded that the a-Si had p-type character from the better rectification, observed in the case of the a-Si/n-type c-Si heterojunction as compared to the a-Si/p-type c-Si heterojunction. The same results had some years earlier found for amorphous germanium on crystalline silicon heterojunctions [2]. From capacitance–voltage (C–V) characteristics of this heterojunctions, the authors deduced an acceptor density in the a-Si of 10^{16} cm^{-3} . Only few years later, good rectification has been obtained on a similar structure and, using capacitance–voltage measurements for the electrical characterization, a rather high built-in-voltage of 0.7 V has been measured [3]. The authors attributed the improved characteristics to a better interface, obtained by heating under vacuum conditions of the crystalline silicon substrate to 400 °C prior of the amorphous silicon deposition. More than 20 years later, in situ transient microwave conductance (TRMC) measurements during heating and cooling of crystalline silicon wafers confirmed the importance of the c-Si substrate heating before amorphous silicon deposition, measuring directly the change in the minority carrier lifetime during this heat treatment [4]. In 1974, the first deposition of hydrogenated amorphous silicon on crystalline silicon has been reported by Fuhs et al. [5], resulting in an amorphous silicon top layer with a lower defect density, where electrical transport in the amorphous layer was not anymore dominated by variable-range hopping [6]. It should be noted that a series of other types of amorphous semiconductor on crystalline silicon heterojunctions have been investigated in these early years, for example, with amorphous germanium [2], amorphous oxides [7], and amorphous chalcogenides [7] as top layers. Photovoltaic effects observed on these devices are already mentioned in [8]. A detailed analysis of the current transport mechanisms in intrinsic amorphous silicon on crystalline silicon heterojunction and a detailed comparison with Schottky diodes have been given for the first time by Brodsky et al. [8]. The authors discussed already the difference of the barrier heights depending on the

substrate doping polarity and found a higher barrier for the a-Si/p-type c-Si junction. In the beginning, all a-Si/c-Si heterojunctions have been realized using intrinsic amorphous silicon either on n-type or on p-type Czochralski grown crystalline substrate. Only in 1975, the possibility of a substitutional doping of amorphous silicon has been demonstrated [9]. In the following years, the actually still-used multitunneling capture-emission model, regarding the electronic transport over at the heterojunction in an i-a-Si:H on p-c-Si with different c-Si resistivities, has been developed by Matsuura et al. [10], based on C-V and temperature-dependent dark I-V measurements. Often, as already mentioned for the first publications, the heterojunction has been just used to determine the material parameters of the amorphous silicon top layers, as for example using C-V measurements, an intrinsic a-Si:H on n-type crystalline silicon structure by Sasaki et al. [11]. Similar measurements, but in a MOS configuration, have been performed later, where the highly doped c-Si substrate served just as gate electrode and for the growth of a high-quality thermal oxide [12]. First industrial applications of the heterojunction focused on the vidicon operation and in this case, indeed, a top intrinsic amorphous silicon layer is required in order to avoid lateral current transport and hence "blooming" effects [13].

Some years later, however, a strong interest in photovoltaic applications of the a-Si:H/c-Si heterojunction emerged. Initially, n-type a-Si:H on p-type polycrystalline silicon as low-cost double-junction cells with a nip a-Si:H top cell [14] (cf. Fig. 3) or a-Si:H/ribbon c-Si as bottom cell of a TANDEM solar cell with a top pin-a-Si:H junction [15] has been realized. In the case of the TANDEM device, a three-terminal configuration has been chosen in order to avoid the top/bottom cell current matching problem and an initial efficiency of 11 % has been reported.

In this early period, all photovoltaic a-Si/c-Si heterojunction devices are n-type amorphous on p-type (poly)crystalline devices. As mentioned earlier, the importance of the interface preparation for this kind of heterojunction was already taken into account in a very early stage [3]. More emphasis on the interface recombination influence on the device properties has been given in the moment, when specific characterization tools have been developed. In particular, the application of the contactless (TRMC) technique [16] as in situ technique first for the characterization of a-Si:H layer growth on glass substrates [17, 18] and then on crystalline silicon substrates [19] enabled the monitoring of the interface recombination during the growth of the amorphous layer. In the case of the monitoring of the heterojunction formation, initially a strong damaging of the crystalline silicon substrate due to the plasma process, followed by a successive passivation during a-Si:H growth, has been observed [19, 20]. The combination of the in situ TRMC technique with in situ spectrally resolved ellipsometry enabled, at the same time, a monitoring of the electronic properties and of the structural evolution of the c-Si surface during plasma processing [21]. Another result of the in situ TRMC-measurements is the direct observation of the charge carrier injection from the amorphous layer into the crystalline silicon substrate. In particular, the dependence

Fig. 3 **a** Cross-sectional view of the tandem solar cell by Okuda, Okamoto, and Hamakawa. **b** Schematic band diagram [14]. Copyright 1983 The Japan Society of Applied Physics



of the injection efficiency on the a-Si:H bulk layer and interface properties has been investigated [22] and correlated with the electrical characteristics of the finished heterojunction device [23]. Due to the knowledge that amorphous silicon layers are as efficient as SiO_2 layers for the surface passivation of crystalline silicon substrates, as determined again by the TRMC technique [24]. In 1992, a new type of a-Si:H/c-Si heterojunction solar cell has been presented by Sanyo—namely the HIT solar cell, the p-type amorphous on n-type crystalline silicon solar cell with a thin intrinsic interface layer [25]. Already, the first publications reported 18.1 % conversion efficiency (30), and nowadays, 23.0 % have been achieved for a large-area (100 cm^2) HIT solar cell [26] (note that Sanyo uses the acronym HIT, “Heterojunction with Intrinsic Thin layer,” for its heterojunction solar cells).

1.3 Economic Aspects

It might be helpful to start this chapter with a brief survey on the photovoltaic installations. Figure 4 shows the repartition of the power production for Germany, the rest of Europe, and the rest of the world [27].

A more detailed picture is obtained when looking at the annually installed power. An example is found in Fig. 5 for the year 2008 [28].

The interesting point in this figure is the absolute numbers in some segments. Spain, for example, has installed a capacity of 2,400 MW which is more than the

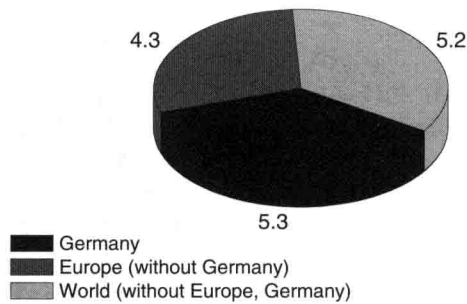


Fig. 4 Repartition of the total installed solar power (in GW) up to 2009

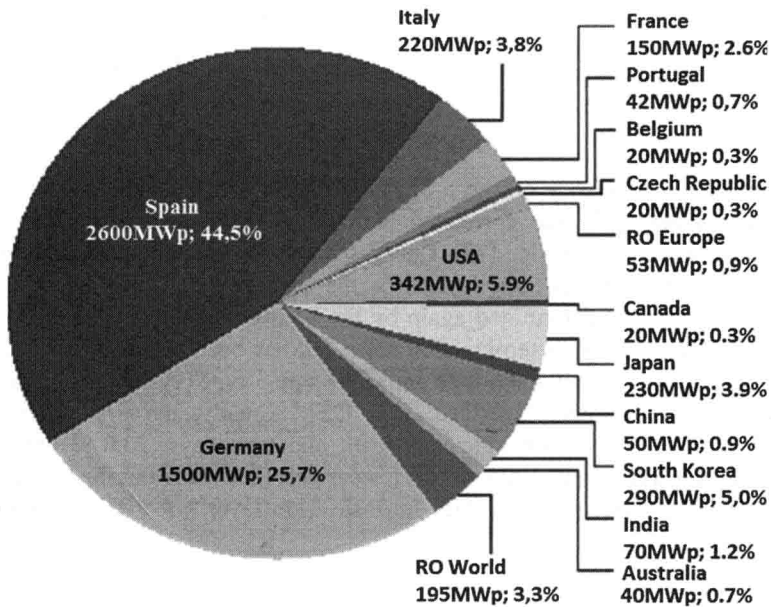


Fig. 5 Worldwide installed solar power in 2008

Table 1 Technical data of a typical Sanyo module [31]

Maximum power (P_{\max})	225 Wp*
Voltage at maximum power point (V_{mp})	33.9 V
Current at maximum power point (I_{mp})	6.64 A
Open-circuit voltage (V_{oc})	41.8 V
Short-circuit current (I_{sc})	7.14 A
Power tolerance	+10/−5 %
Maximum system voltage	1,000 V
Dimensions (L × W × H, mm)	1,610 × 861 × 35 mm
Weight	16.5 kg
Performance guarantee	20 years for 80 % of the minimum power
Product guarantee	2 years

output of the Three Miles Island Reactor with an output of 800 and 900 MW of both blocks. It is anticipated that the 2020 installation will amount to 44 GW resulting in accumulated power of 269 GW.

This situation is reflected in the field of heterojunction solar cells. Because Sanyo Company is the only commercial supplier, it is sufficient to use its production data. While in 2009, 340 MW are anticipated, this number will increase to 2 GW in 2020 [29, 30].

Finally, we reproduce some technical data of a typical heterojunction module (Table 1).

It is clearly seen that its minimum efficiency of 16.2 % is one of the best of all commercially available modules. A further advantage consists in the fact that heterojunction modules exhibit a lower open-circuit voltage temperature coefficient (<-1.78 mV/K) than crystalline modules (-0.2 mV/K) [32, 33]. This coefficient essentially determines the temperature coefficient of the efficiency. Recently, Sanyo has repeated these measurements and given more precise data. Temperature coefficients of -0.5 and -0.3 %/K for crystalline and HIT solar cells, respectively, were given [34].

2 Useful Material Parameters

2.1 Useful Data of Monocrystalline Silicon

The crystal structure of the most frequently used semiconductor material, namely monocrystalline silicon, is that of the diamond lattice. It is arranged in the form of two interwoven face-centered cubic lattices with one silicon atom placed on each lattice point [35] (Table 2, Fig. 6).

The two elementary cells are displaced against each other by a quarter of the body diagonal. The bonds are purely covalent.

Monocrystalline silicon is an indirect semiconductor. The resulting absorption coefficient is seen in Fig. 7.

Table 2 Some material properties of crystalline silicon [35, 37]

<i>Crystal properties</i>	
Atoms/cm ⁻³	5.0×10^{22}
Atomic weight	28.09
Density (g/cm ³)	2.24
Melting point (°C)	1,415
Vapor pressure (Pa)	1 at 1,650 °C, 10 ⁻⁶ at 900 °C
<i>Thermal properties</i>	
Coefficient of thermal expansion (°C ⁻¹)	2.6×10^{-6}
Specific heat (J/g × °C)	0.7
Thermal conductivity (W/cm × °C)	1.5
Thermal diffusion coefficient (cm ² /s)	0.9
<i>Dielectric properties</i>	
Dielectric constant	11.9
<i>Electric properties</i>	
Bandgap (eV)	1.12
Intrinsic carrier concentration (cm ⁻³)	1×10^{10}
Intrinsic Debye length (μm)	24
Intrinsic specific resistivity (Ω cm)	2.3×10^5
Effective state density in the conductance band, N_c (cm ⁻³)	2.8×10^{19}
Effective state density in the valence band, N_v (cm ⁻³)	1.04×10^{19}
Electron affinity, χ (V)	4.05
Breakdown voltage (V/cm)	$\approx 3 \times 10^5$
Minority carrier lifetime (s) (intrinsic material)	2.5×10^{-3}
Drift mobility (cm ² /V × s) electrons/holes	1500/450

Fig. 6 Lattice structure of the silicon and the diamond lattice

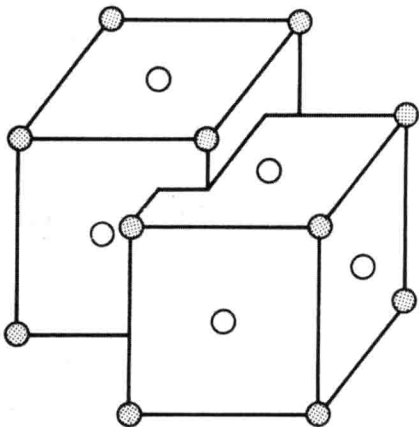


Table 1 shows a compilation of some silicon data subdivided according to crystalline, thermal, electric, and dielectric properties. As to the temperature-dependent characteristics such as thermal conductivity and dielectric properties, room temperature (300 K) is assumed.